Quantum Electronics **50** (8) 742–749 (2020)

https://doi.org/10.1070/QEL17371

Scheme for stabilising the phase and arrival time of ultrashort laser pulses in a coherent beam combining fibre system

A.V. Andrianov, A.P. Korobeynikova

Abstract. **An algorithm has been demonstrated for simultaneously measuring the phase and arrival time of optical pulses relative to pulses in a reference channel using one detector array. Based on this algorithm, a simple optoelectronic pulse phase and arrival time stabilisation scheme has been designed for operation in a coherent beam combining fibre system for ultrashort pulses (including chirped ones). We have studied the performance of the stabilisation scheme. In particular, we have reached a phase measurement rate of 25 000 cps, demonstrated an ~2 kHz limiting phase stabilisation frequency in a feedback loop, and obtained an arrival time measurement accuracy of ~5% of the transform-limited pulse duration at a measurement rate of 5 cps. In experiments concerned with coherent beam combining for two channels of a pulsed fibre system at a wavelength of 1030 nm, we have demonstrated phase stabilisation with an accuracy better than λ/100 and delay setting accuracy of 10 fs at a transform-limited pulse duration of ~200 fs and obtained 94% beam combining efficiency.**

Keywords: *coherent beam combining, optical phase detector, ultrashort laser pulses, active phase stabilisation.*

1. Introduction

Multichannel coherent beam combining laser systems have attracted a great deal of attention because they allow the power and energy of laser radiation to be increased many times. The ability to raise optical power is of particular importance for femtosecond and fibre laser systems, where nonlinear effects and optical breakdown play a critical role. To overcome these limitations, ideas of building a system based on a multichannel fibre amplifier whose output beams are coherently combined are widely discussed and investigated [1–5]. The inevitable influence of temperature variations, vibrations, and acoustic noise leads to random fluctuations of the relative phase of light between the channels of the laser system. Therefore, a scheme for stabilising the relative phase of the light beams to be combined is needed for effective coherent beam combining. The combining of broadband and ultrashort pulses, which is the subject of major attention in this study, poses an additional problem: to equalise and stabilise the pulse arrival time [4, 5]. The accuracy needed in maintaining the phase is determined by requirements for total optical power stability and is usually 0.01–0.1 of the wavelength used. The necessary accuracy in equalising the pulse arrival time is ~0.1 of the pulse duration [4, 5].

The implementation of coherent ultrashort pulse combining in fibre systems has been the subject of extensive studies. Special mention should be given to the ICAN and XCAN projects [6, 7], aimed at demonstrating beam combining for a large number of chirped pulse fibre amplifiers (about 100 as an intermediate step and tens of thousands in the longer term), followed by compression of the resultant beam pulse to a femtosecond duration in a compressor.

Following a general concept, we are also designing a coherent beam combining system based on a femtosecond master oscillator emitting at a wavelength of ~1 μm, a multichannel fibre splitter, and an array of ytterbium-doped fibre amplifiers whose output signals will be combined using a tiled aperture configuration. In our system, in addition to beam combining into one beam we plan to examine the feasibility of synthesising various sum field configurations by controlling the amplitude and phase of individual beams. This requires a specially designed phase detection and locking scheme with the possibility of independently setting the target value of the phase in each channel throughout the range $0-2\pi$. The amplitude in the channels of our system will be varied by changing the pump power in the output stages of the multichannel amplifier, which will lead to changes in the thermal conditions of their operation and, hence, to noticeable changes in pulse arrival time. This requires the development of a pulse arrival time measurement and stabilisation system. A device that allows these issues to be resolved should be sufficiently fast, simple, and cheap to be replicated for many channels.

In this paper, we present algorithms for simultaneous pulse phase and arrival time measurements using one detector, propose an effective engineering implementation of an optoelectronic device for stabilising the pulse parameters using these algorithms, and examine its characteristics as exemplified by a low-power coherent beam combining system for two fibre channels. Owing to their simple engineering implementation, we plan to use an array of such detectors for making a high-power multichannel coherent beam combining system.

It is worth noting that there are beam-phasing schemes in which beam phases are not measured. In such schemes, the only parameter to be measured (objective function) is the combined beam intensity, and necessary phase compensation values (and the corresponding control signals to phase modulators) are adjusted using an iterative algorithm (e. g. the gradient descent method [8]) for maximising the objective function. However, this approach is unsuitable for directly finding

A.V. Andrianov, A.P. Korobeynikova Institute of Applied Physics (Federal Research Centre), Russian Academy of Sciences, ul. Ulyanova 46, 603950 Nizhny Novgorod, Russia;
e-mail: alex.v.andrianov@gmail.com

Received 18 May 2020
Kvantovaya Elektronika **50** (8) 742–749 (2020)
Translated by O.M. Tsarev

the sought phases of individual beams. There is a method for measuring relative phases in channels that also requires only a single-element detector of the combined beam intensity. The method relies on an intentional introduction of a small phase modulation into each channel at its unique frequency (so it is referred to as frequency tagging) [9]. Using digital processing of the detector signal, one can separately assess the contribution of each channel and reconstruct its phase. At a large number of channels, the required modulation frequency becomes comparable to the pulse repetition rate, which makes the method difficult to scale up. A drawback common to the above methods is that the time delay of pulses cannot be measured.

The most direct method of measuring the phase and arrival time of signals in coherent beam combining systems is based on the observation of their interference with a reference beam signal. The method uses one dedicated channel, and the pulse phase and time delay in the other channels are measured relative to those in this channel. Based on this method, we constructed an algorithm and proposed an engineering implementation of a scheme that allows one to measure both the phase and time delay of a signal relative to those of a reference beam signal and is suitable for stabilising these parameters in a coherent beam combining system. Characteristic frequencies of phase fluctuations depend on particular implementation, but in the case of fibre systems similar to that being designed by us they range up to several kilohertz [10–13]. Significant pulse delay fluctuations have a rather long characteristic timescale because they are caused primarily by thermal effects. Because of this, the operation rate of the phase stabilisation system is of key importance for the operation of the feedback loop in a coherent beam combining system.

2. Optical scheme of the detector

Consider first the scheme of a detector (Fig. 1a) that allows one to measure only the phase of a signal relative to that of a reference beam signal. The test and reference beams are combined in a beam splitter and directed to the detector of the beam intensity, which depends on the phase difference between the beams. In the simplest configuration with a single-element detector, there is an ambiguity in phase determination: the detector signals at phase differences φ and $2\pi - \varphi$ are identical. To eliminate the ambiguity, we use a configuration in which the beams intersect at the detector input at a small angle, producing an interference fringe pattern. From the shift of the fringes, one can uniquely determine the phase of the test beam relative to that of the reference beam. Figure 1a shows a schematic of this optical detector.

To observe the interference pattern, a detector array and an algorithm for reconstructing the phase from the shift of the interference fringes is needed. At first sight, this complicates the system, but with a proper choice of elements the scheme can be made simple and cheap, comparable in the number and cost of elements to the scheme with a single-element detector. Besides, the scheme with a detector array offers significantly greater signal processing possibilities. Note that a phase detector based on an interference principle with the use of a CCD camera as an optical sensor was considered in a number of studies [10–12].

To ensure the possibility of measuring the pulse delay relative to a pulse in the reference channel, the detector configuration can be modified so that interference of light beams decomposed into a spectrum is observed at the detector input (Fig. 1b). The reference and test beams can then be parallel to each other. Just behind the beam splitter, we place a mask with slits that coincide with the centres of the test beams and act as monochromator entrance slits. The rest of the scheme is the simplest spectrometer consisting of a diffraction grating and two lenses, which transfers the image of the beams after the mask to the detector array, with decomposition into a spectrum along the transverse coordinate. It is worth noting that, in the case of a multiple-beam system, one lens system and one diffraction grating with an appropriate aperture can be used.

We take the test and reference light pulses to have identical spectral amplitudes described by the complex function $A(\omega)$, where ω is the optical frequency. If the test pulse has a phase shift φ and time delay T relative to the reference pulse, its spectral amplitude can be written in the form

$$S_1 = A(\omega)\exp(\mathrm{i}\omega T + \mathrm{i}\varphi). \quad (1)$$

The light intensity at the detector input can be approximately represented as

$$I(x) \propto |A(\alpha x)|^2 |1 + \exp(\mathrm{i}\alpha x T + \mathrm{i}\varphi)|^2, \quad (2)$$

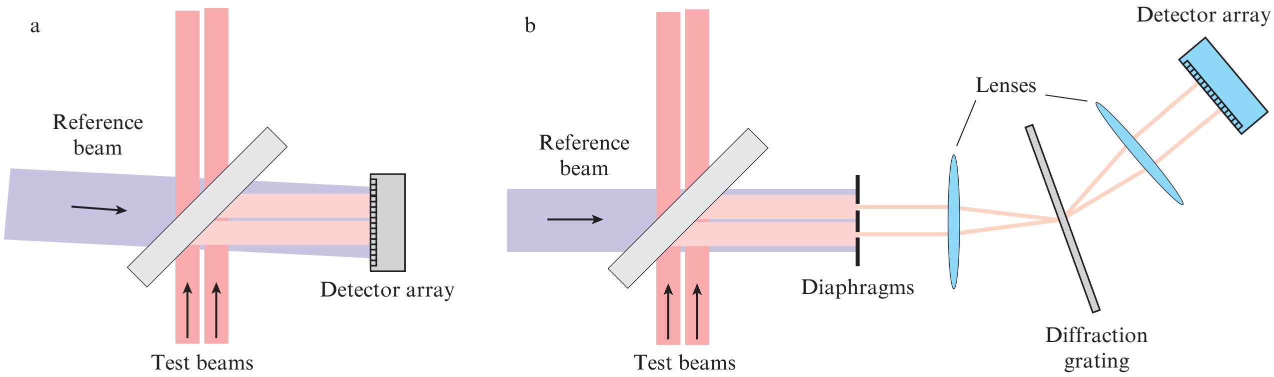

Figure 1. (a) Schematic of the detector for measuring the phase of several beams relative to that of a reference beam and (b) modified configuration that allows one to additionally measure the time delay of signal pulses relative to the reference pulse.

where α is the scale factor relating the spatial coordinate x and frequency ω (and determined by the diffraction grating and lenses). If necessary, the scale factor can be found after appropriate calibration of the scheme.

It follows from (2) that the interference pattern at the detector input is formed by interference fringes whose spacing depends on time delay T and whose shift along x depends on the phase difference φ. This allows both parameters to be determined concurrently from one measurement with the detector array. Note that the absolute values of T and φ of course depend on many factors, but for a feedback system only the ability to maintain these parameters near some reference values is important. The interference fringe spacing optimal from the viewpoint of subsequent processing can be set using a time shift of the reference pulse by some value T_0. It is worth noting that there is an alternative approach to arrival time determination, based on measurement of the phase difference between the test and reference beams at two distinct wavelengths using two phase detectors [13]. This method requires using sufficiently narrow band filters and twice as many detectors, which makes it more complex from the viewpoint of practical implementation.

It should be emphasised that the proposed measurement algorithm is suitable for any pulse duration and spectral phase (including highly stretched and chirped pulses) provided the reference and test signals have identical phases, which follows from (2) and allows a detector based on our algorithm to be placed before the pulse compressor. This distinguishes our algorithm from methods based on nonlinear processes (e. g. on maximising the intensity at the sum frequency of the reference and test beams), which are only operative for compressed pulses and cannot be directly used for long chirped pulses. The relative accuracy of our algorithm (the ratio of the time shift measurement uncertainty to the transform-limited pulse duration) is independent of the pulse duration and emission bandwidth, which can be achieved by adjusting the scale factor α.

3. Electronic scheme of the detector

Analysis of various electronic components led us to choose an approach allowing a feedback scheme with a high operation rate and significant flexibility and easy to scale up to many channels to be produced using a very small number of cheap elements. Required elements are ordinary and, hence, readily available, cheap, and reliable.

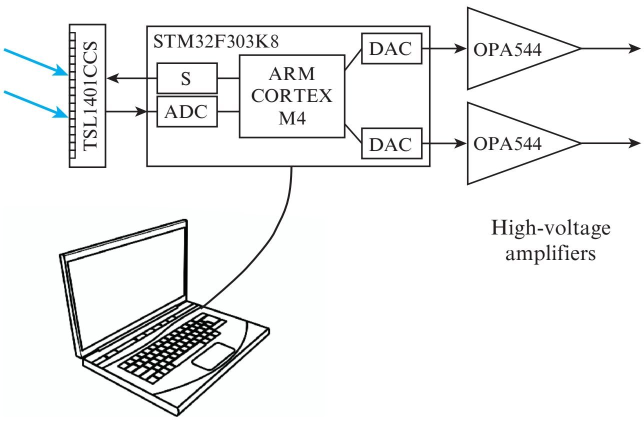

Figure 2. Schematic of the detector for measuring the phase and time delay of optical pulses (S = synchroniser).

Figure 2 shows a schematic of the electronic system. The system is intended for operation in a coherent beam combining scheme, so it needs feedback algorithm implementation and outputs for controlling an actuator with the aim of phase tuning. The actuator used is a piezoelectric plate with optical fibre cemented to it. A voltage applied to the plate leads to stretching of the fibre, thereby allowing the pulse phase and delay to be controlled.

The scheme comprises an optical detector array, microcontroller, and two high-voltage amplifiers producing a feedback signal to the piezoelectric elements. Note that one unit of the detector is intended to operate simultaneously with two channels completely independent of each other.

As a detector array, we used TSL1401CCS, a widespread linear array sensor. This supercompact linear array (8.8 × 1 mm in dimensions) is sensitive at wavelengths of up to ~1.09 μm and has 128 sensor elements 64 × 64 μm in dimensions, a built-in control signal generation scheme, and a preamplification system. Its distinctive feature is the ability to operate at a rather high frequency, up to 30 000 full 128 pixel frames per second. Since we are designing a scheme for simultaneous operation with two channels, the sensitive area of the optical sensor is divided into two parts with 64 pixels for each channel.

Information processing and feedback algorithm implementation are ensured by an STM32F303K microcontroller (STMicroelectronics), which includes all necessary components [fast analogue–digital converter (ADC), hardware core, and two digital–analogue converters (DACs)]. The controller is cheap and compact and requires a minimum number of external electronic elements.

The scheme operates as follows: An optical signal (the interference pattern of the test and reference beams) falls on the linear array sensor. The analogue signal from the linear array is fed directly to the ADC of the microcontroller, where it is digitised. Next, program processing of the signal is performed. The image on the linear array has a smooth envelope and interference oscillations. To find the phase of the interference oscillations, the following algorithm is used: At the ADC output, a digitised signal is produced, whose discrete values we denote as a_n ($n = 1, ..., N$, where $N = 64$ is the number of pixels per channel). Two sums equivalent to numerical integration are calculated:

$$S = \sum_{n=1}^{N} a_n s_n, \quad C = \sum_{n=1}^{N} a_n c_n. \tag{3}$$

Here, s_n and c_n are quadrature functions, which can be taken in the form

$$s_n = \exp[-p(n - N/2)^2]\sin(qn),$$
$$c_n = \exp[-p(n - N/2)^2]\cos(qn), \tag{4}$$

where p and q are coefficients chosen based on the form of the function being measured. Next, the phase of the test beam relative to the reference beam can be calculated as $\varphi = \arctan(S/C)$. In our system, we need phase stabilisation near a preset value, ϕ (which can take any value from $-\pi$ to π), so to avoid operation near discontinuities of the function

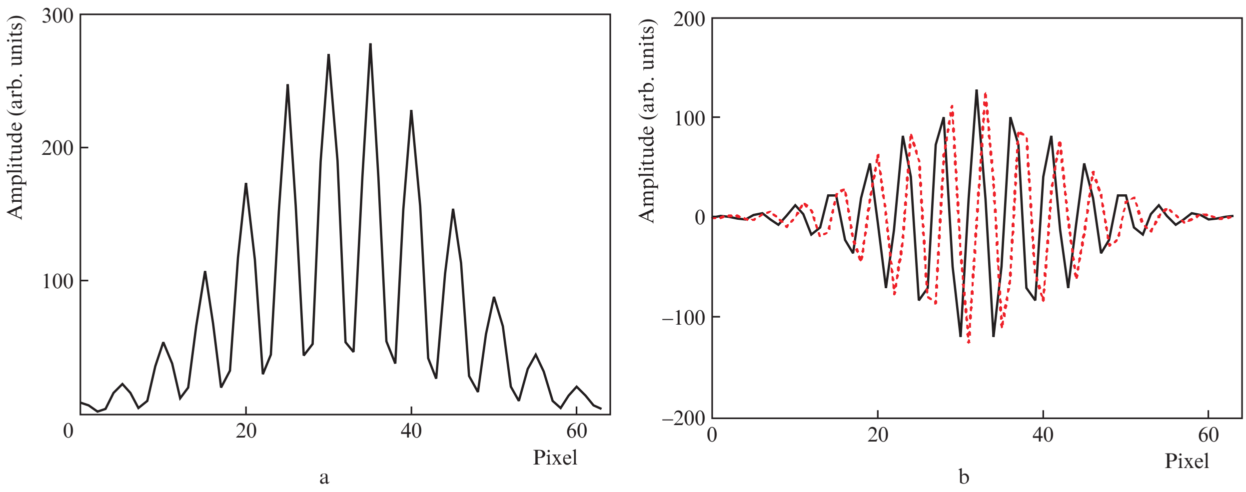

Figure 3. (a) Interference pattern detected by a sensor and (b) quadrature functions c_n (solid line) and s_n (dashed line).

arctan(S/C) it is more convenient to calculate at once the difference between the measured phase and its target value:

$$\varphi - \phi = \arctan\left(\frac{S\cos\phi - C\sin\phi}{C\cos\phi + S\sin\phi}\right). \quad (5)$$

The choice of the sine and cosine as quadrature functions, with an additional Gaussian envelope, which falls off essentially to zero at the grid edge, is dictated by the necessity to eliminate the influence of image edges. Figure 3 presents an example of measured images and quadrature functions.

The proposed phase measurement algorithm is extremely excessive in terms of input data and, accordingly, rather noise-resistant and insensitive to a decrease in the amplitude of the entire signal and individual pixels and to the interference fringe visibility.

The instantaneous phase is used at the input of the program algorithm of a proportional – integral – derivative (PID) controller [14], which generates feedback signals. The signals are converted to a control voltage by DACs built into the controller and are fed directly to a high-voltage amplifier. The amplified voltage is applied to the piezoelectric fibre stretchers [15, 16]. The rate of processing of full frames from the linear array sensor is about 30 000 frames per second, and the measured response time of the scheme (between a change in the phase of the optical signal and the arrival of the response to the piezoelectric element) is ~ 40 μs. This allows a feedback bandwidth of up to several kilohertz to be reached [14], which is of importance for suppressing high-frequency vibrations and acoustic noise. Spectral characteristics of noise suppression are examined in Section 4. Note that systems with a kilohertz noise suppression band are being developed by the world leading groups for combining a large number of femtosecond light beams at the output of fibre channels [11, 12].

The feedback system allows the phase difference between the signal and reference beams to be maintained at the level of a preset value, ϕ. The change in optical path length, compensated for by the piezoelectric element, can then reach a large number of wavelengths (up to ~20 in our case). For the system to be able to operate after the control limit of the piezoelectric elements is reached, we implemented a 'relief' algorithm, which consisted in returning the control signal to the control range by changing (increasing or decreasing) it by a value equivalent to a change in optical path length by an integer multiple of the wavelength (twice the wavelength in our case).

In an ideal case, as a result of phase stabilisation the total optical path length in the channel remains unchanged and, hence, the pulse arrival time also automatically remains stable. However, even a short error in phase determination or a brief synchronisation loss, which may be caused by a sharp change in operation conditions (e. g. when one of the channels is switched off and on or as a result of a very abrupt external influence), will lead to an unremovable arrival time mismatch accumulation. Moreover, after the system is switched on and its thermal conditions are stabilised, it is necessary to equalise the arrival time in its channels. For this purpose, we use the spectral interference detector configuration schematised in Fig. 1b and a specially designed algorithm. In this configuration, each frame from the linear array sensor carries information about both the signal phase and pulse delay. However, as mentioned above, considerable changes in arrival time occur far more slowly than fast but small changes in phase. This allows one to evaluate the arrival time (which requires a more complex algorithm) much more rarely. Because of this, the calculation algorithm was implemented not on a microcontroller but on a control personal computer. It follows from relation (2) that, to find the pulse delay, it is sufficient to determine the spectral interference fringe spacing. This could be done using a simple algorithm based on calculation of the fast Fourier transform of the measured signal, with a mask in the form of a Gaussian pulse superimposed on it to exclude the effect of the image edges. Next, the maximum of the magnitude of the Fourier spectrum was found, and the result was used to calculate the pulse delay T.

The proposed detector configuration can readily be scaled up for handling many channels. It may seem that the scheme utilising the sensor array and microcontroller is too complicated. However, even the simplest single-element detector (one photodiode per channel) requires at least a preamplifier and ADC (even if data processing and feedback algorithm implementation in all channels are ensured by a single powerful computer). This makes our scheme comparable in cost and

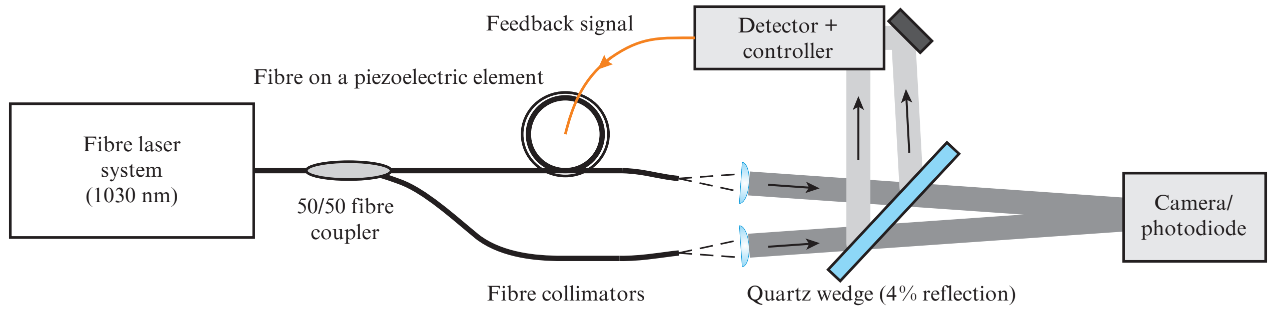

Figure 4. Schematic of the experimental setup for testing the phase stabilisation and coherent beam combining scheme.

complexity to the simplest detector, while it offers considerably greater possibilities.

4. Experimental results

Figure 4 shows a schematic of our experimental setup. A pulsed optical signal with a centre wavelength of 1.03 μm was generated by the front end of a fibre-optic system similar to that described previously [17, 18]. It included a 1.03-μm master oscillator, fibre stretcher, and one ytterbium-doped polarisation-maintaining fibre preamplifier stage. The system generated ~50-ps chirped light pulses with an average power of 90 mW, repetition rate of 49 MHz, and spectral bandwidth of ~8 nm, which could be compressed to ~200 fs. The pulses were separated into two channels by a symmetric fibre coupler. One of the channels included a piezoelectric phase modulator. The linearly polarised beams from the output of the fibres were collimated by aspherical lenses (fibre collimators) and propagated at a small angle between them. Part (about 4%) of each beam was tapped by a quartz wedge and directed to the detector designed by us. One of the channels was taken to be a reference. To test the possibility of coherent combining, the beams transmitted through the wedge were intersected at some point, where the total intensity was monitored with a CCD camera (to adjust the beam intersection) or photodiode (to control the operation of the phase stabilisation scheme). The output fibres were single-mode, which ensured good quality of the (nearly Gaussian) collimated beams. In such a case, any region of the beam can be chosen for operation of the detector and phase stabilisation scheme, and stabilisation is ensured automatically over the entire beam aperture.

First, we tested the detector configuration that allowed us to measure only the signal phase (Fig. 1a). The time dependence of the signal phase measured by our detector without feedback in the system is presented in Fig. 5a. It is seen that phase fluctuations have various timescales and exceed 2π. In plotting these data, we used a phase unwrapping algorithm which eliminated discontinuities if phase changes exceeded 2π. The algorithm analyses the difference between the current and preceding phases. If $\varphi_n - \varphi_{n-1} < -\pi$ ($\varphi_n - \varphi_{n-1} > \pi$), 2π is added to (subtracted from) the output value. During the operation of the algorithm, this contribution increases. Note that, if the detector operates in the feedback loop, there is no need for phase unwrapping because the difference between the measured phase and its target value, calculated using Eqn (5), is always near zero. From the measured phase fluctuations, we calculated the combined signal intensity, which was compared to that measured by an independent detector (Fig. 5b). The observed agreement between the results of these independent measurements confirmed that our detector was linear over the entire range of phase changes, from zero to 2π.

Figure 6a shows a characteristic phase noise spectrum obtained without the feedback system. It is seen that fluctuations occur mainly at frequencies below a few tens of hertz,

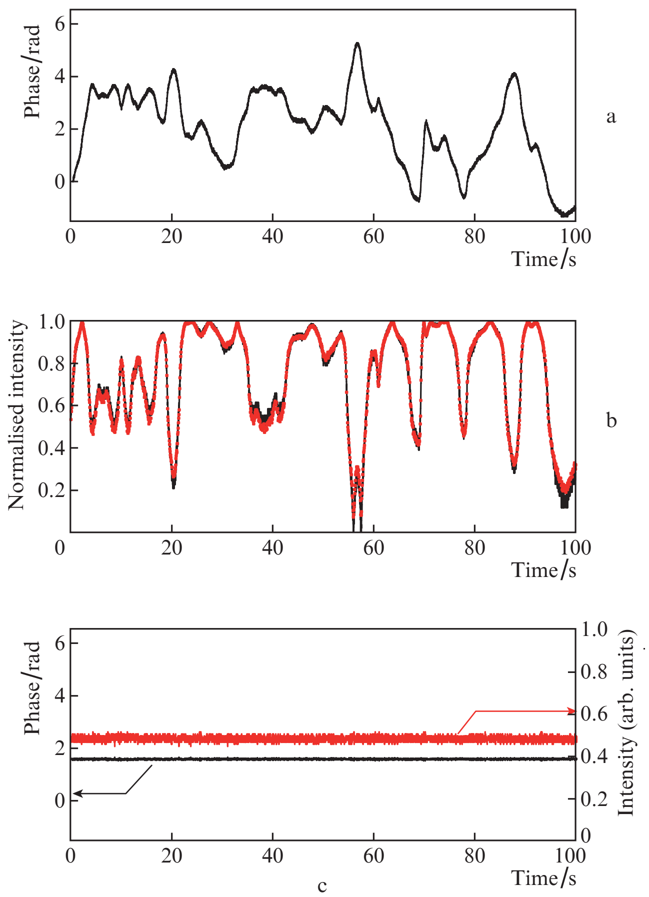

Figure 5. (Colour online) (a) Signal phase measured without feedback, (b) coherent beam combining signal intensity calculated from the measured phase (black solid line) and measured by an independent detector (red dotted line), (c) signal phase measured with feedback (black solid line), and combined signal (red solid line).

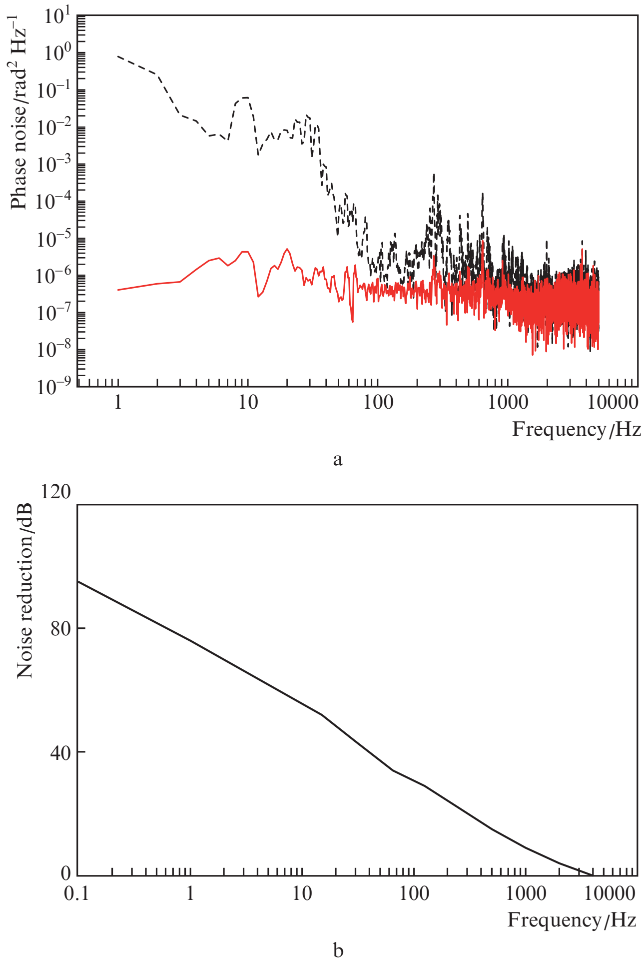

Figure 6. (a) Phase noise spectra obtained without (dashed line) and with (solid line) feedback and (b) noise reduction factor as a function of frequency.

but the spectrum contains noticeable peaks at frequencies of up to ~1 kHz, which we believe are due to acoustic noise and high-frequency vibrations. In our system, they are presumably generated by the cooling fans of the diode pumping systems and other devices and can be augmented as a result of resonance with elements of the laser system housing. We purposefully did not take any vibration isolation or noise suppression measures in order to demonstrate the performance of the stabilisation system.

Next, the feedback loop was included in the system using a PID algorithm operating on the same microcontroller as the phase detection algorithm. Figure 5c shows the time dependence of the phase measured with the feedback system. It is seen that the phase remains stable throughout the measurement time. An independent stability assessment was made using a photodiode placed in the interference pattern region between the minimum and maximum of one of the interference fringes (i. e. in the region of the highest sensitivity to fluctuations). The photodiode signal is also shown in Fig. 5c. The standard deviation of residual phase fluctuations measured directly by the phase detector was 0.04 rad, and that estimated from the photodiode signal was 0.06 rad. In any case, this corresponds to phasing accuracy better than $\lambda/100$.

The phase noise spectrum obtained with the stabilisation system switched on (Fig. 6a) demonstrates effective phase fluctuation suppression up to kilohertz frequencies. For more regular testing of the stabilisation scheme, we used a standard method based on an intentional phase modulation via the addition of a tunable-frequency harmonic signal to the voltage applied to the piezoelectric element. Note that its resonance frequency is above 10 kHz, i. e. its response in the frequency range of interest for us can be thought to be essentially instantaneous (which was checked without the feedback system).

Figure 6b shows the phase fluctuation reduction factor as a function of frequency. It is seen that our scheme operates at frequencies of up to ~2 kHz. This is more than sufficient for compensating all noise, and we expect that the coherent beam combining system being developed by us will be capable of operating not only under ordinary laboratory conditions but also in the presence of noise and vibration sources. The broad frequency band of stabilisation can be especially important for promising designs of coherent combining systems for the output of amplifiers operating in a highly nonlinear regime, where intensity fluctuations translate into phase fluctuations [19–21].

Next, we tested the detector configuration that allowed us to additionally measure the pulse arrival time (Fig. 1b). Note that the phase detection algorithm remained unchanged in this case and worked successfully as well.

To test the pulse arrival time detector, a small known delay in the range from –250 to +250 fs, with an uncertainty of ~6 fs, was intentionally introduced into one of the channels (the fibre collimator in this channel was shifted along its axis on a motorized micrometer positioning stage). Figure 7 shows the reconstructed delay and the value evaluated form the displacement of the collimator. The measurements were made at constant collimator displacements whose difference corresponded to a pulse shift by 50 fs. During displacement, the phase stabilisation was switched off to avoid delay self-compensation. At each point, 100 measurements were made, without additional averaging. The standard deviation of the measured delays from the evaluated ones was ~10 fs. Thus, the relative accuracy in our delay measurements was ~0.05 (10 fs/200 fs). This was sufficient to ensure combining efficiency above 95% [4]. The measurement frequency was 5 Hz and was limited by the rate of data transfer from the microcontroller to the computer by an unoptimised protocol. It could be raised to tens of hertz.

It should be emphasised that the algorithm implemented using spectral interferometry allows the sign of the time delay to be determined, as distinct from methods that maximise the spatial interference pattern visibility [12] or nonlinear response (second harmonic signal from combined beams), which provide information only about the magnitude of time detuning.

Figure 8a shows the intensity profile of one of the beams being combined. At the optimal delay between pulses of the channels, it had a well-defined interference structure (Fig. 8b) with stable position and good visibility of its maxima throughout the beam aperture, pointing to successful operation of the stabilisation system. Coherent combining efficiency, defined as the ratio of the maximum observed intensity in the interference pattern to the maximum possible one at the measured intensities of the beams being combined (Fig. 8c), was 94%. Note that the experiments in question were aimed primarily at examining the operation of the phase and time stabilisation

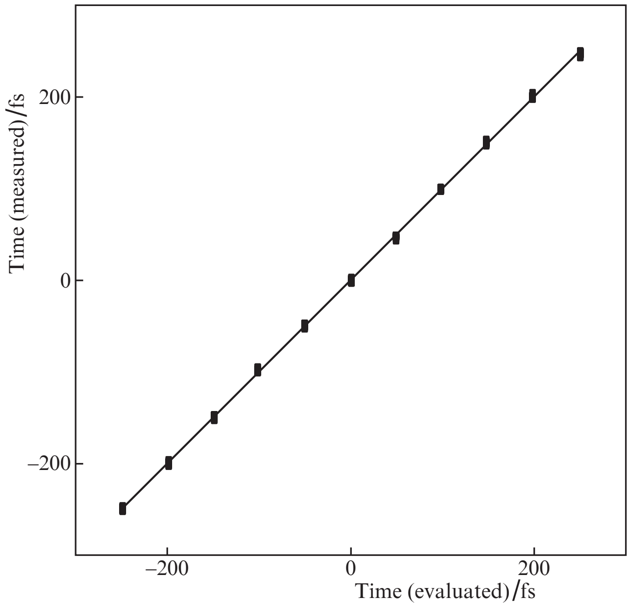

Figure 7. Pulse delays measured by the detector and evaluated using a micrometer positioning stage.

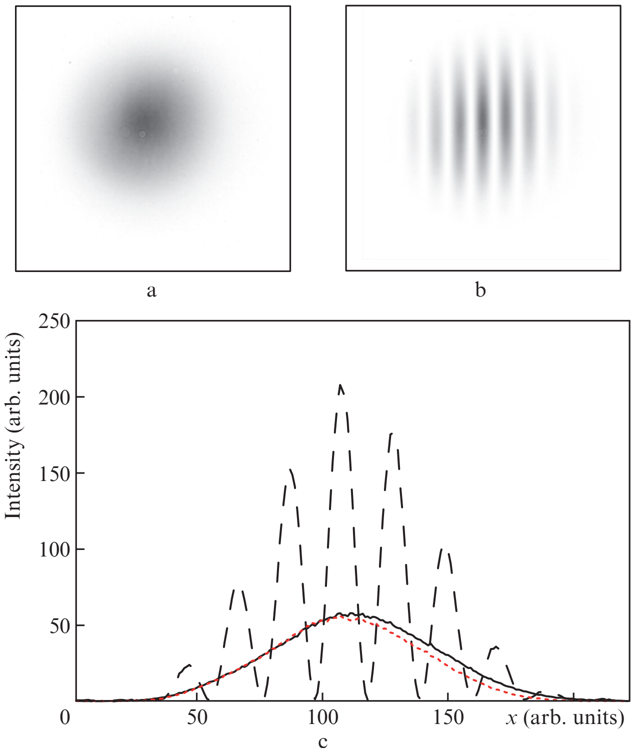

Figure 8. Intensity distributions across one of the beams being combined (a) and the combined beam (b) and intensity profiles integrated with respect to the vertical coordinate for the beams being combined (solid and short-dashed lines) and the combined beam (long-dashed line) (c).

system, rather than at optimising the optical beam combining scheme.

Thus, the proposed detector can be successfully used in a coherent beam combining system.

5. Conclusions

An algorithm has been demonstrated for simultaneously measuring the phase and group delay of optical pulses relative to pulses in a reference channel using one detector array. Based on this algorithm, a phase and group delay stabilisation scheme has been designed for operation in a coherent beam combining system. We have demonstrated a simple engineering implementation of the stabilisation scheme that uses commercially available electronic components and can be scaled up to a large number of channels. The performance of the stabilisation scheme has been studied in experiments concerned with coherent beam combining in a two-channel ytterbium-doped fibre system at a wavelength of 1030 nm. The scheme allows the phase of a signal to be measured and maintained with an accuracy better than $\lambda/100$ and has a limiting stabilisation frequency of $\sim$2 kHz. The effective phase measurement rate is 25 000 cps and the delay measurement rate is 5 cps. The group delay measurement accuracy is $\sim$5% of the pulse duration, which corresponds to 10 fs for 200-fs pulses used in our experiments.

Acknowledgements. A.V. Andrianov is grateful to V.M. Andrianov for his assistance in designing the high-voltage amplifiers for controlling the piezoelectric elements.

This work was supported by the Presidium of the Russian Academy of Sciences (Extreme Light Fields and Their Interaction with Matter Programme) and the RF Ministry of Science and Higher Education (Megagrant, Agreement No. 14.W03.31.0032).

References

1. Fan T.Y. *IEEE J. Sel. Top. Quantum Electron.*, **11**, 567 (2005).
2. Mourou G., Tajima T., Quinn M.N., Brocklesby B., Limpert J. *Nucl. Instrum. Methods Phys. Res., Sect. A*, **740**, 17 (2014).
3. Müller M., Klenke A., Steinkopff A., Stark H., Tünnermann A., *Limpert J. Opt Lett.*, **43**, 6037 (2018).
4. Brignon A. (Ed.) *Coherent Laser Beam Combining* (John Wiley & Sons, 2013).
5. Hanna M., Guichard F., Zaouter Y., Papadopoulos D.N., Druon F., Georges P. *J. Phys. B: At., Mol. Opt. Phys.*, **49**, 062004 (2016).
6. Brocklesby W.S., Nilsson J., Schreiber T., Limpert J., Brignon A., Bourderionnet J., Tajima T. *Eur. Phys. J.: Spec. Top.*, **223** (6), 1189 (2014).
7. Daniault L., Bellanger S., Le Dortz J., Bourderionnet J., Lallier E., Larat C., Mourou G. *Eur. Phys. J.: Spec. Top.*, **224** (13), 2609 (2015).
8. Weyrauch T., Vorontsov M.A., Carhart G.W., Beresnev L.A., Rostov A.P., Polnau E.E., Liu J.J. *Opt. Lett.*, **36**, 4455 (2011).
9. Shay T.M., Benham V., Baker J.T., Sanchez A.D., Pilkington D., Lu C.A. *IEEE J. Sel. Top. Quantum Electron.*, **13**, 480 (2007).
10. Bourderionnet J., Bellanger C., Primot J., Brignon A. *Opt. Express*, **19**, 17053 (2011).
11. Antier M., Bourderionnet J., Larat C., Lallier E., Lenormand E., Primot J., Brignon A. *IEEE J. Sel. Top. Quantum Electron.*, **20**, 182 (2014).
12. Heilmann A., Le Dortz J., Daniault L., Fsaifes I., Bellanger S., Bourderionnet J., Simon-Boisson C. *Opt. Express*, **26** (24), 31542 (2018).
13. Weiss S.B., Weber M.E., Goodno G.D. *Opt. Lett.*, **37**, 455 (2012).
14. Astrom K., Hagglund T. *PID Controllers: Theory, Design, and Tuning* (Instrument Soc. Am., 1995).
15. Gelikonov V.M., Gelikonov G.V., Ksenofontov S.Y., Terpelov D.A., Shilyagin P.A. *Instrum. Exp. Tech.*, **53**, 443 (2010).

16. Zelenogorskii V.V., Andrianov A.V., Gacheva E.I., Gelikonov G.V., Krasilnikov M., Mart'yanov M.A., Mironov S.Yu., Potemkin A.K., et al. *Quantum Electron.*, **44**, 76 (2014) [*Kvantovaya Elektron.*, **44**, 76 (2014)].
17. Andrianov A., Anashkina E., Muravyev S., Kim A. *Opt. Lett.*, **35** (22), 3805 (2010).
18. Bobkov K., Andrianov A., Koptev M., Muravyev S., Levchenko A., Velmiskin V., Kim A. *Opt. Express*, **25** (22), 26958 (2017).
19. Klenke A., Seise E., Limpert J., Tünnermann A. *Opt. Express*, **19**, 25379 (2011).
20. Daniault L., Hanna M., Lombard L., Zaouter Y., Mottay E., Goular D., Bourdon P., Druon F., Georges P. *Opt. Lett.*, **37**, 650 (2012).
21. Andrianov A., Anashkina E., Kim A., Meyerov I., Lebedev S., Sergeev A., Mourou G. *Opt. Express*, **22**, 28256 (2014).